Quasi-periodic States in Coupled Rings of Cells

Fernando Antoneli[a,b,2], Ana Paula S. Dias[a,b], Carla M.A. Pinto[a,c,*]

[a] *Centro de Matemática da Universidade do Porto[1], Rua do Campo Alegre, 687, 4169-007 Porto, Portugal*
[b] *Departamento de Matemática Pura, Faculdade de Ciências da Universidade do Porto, Rua do Campo Alegre, 687, 4169-007 Porto, Portugal*
[c] *Instituto Superior de Engenharia do Porto, Rua Dr António Bernardino de Almeida, 431, 4200-072 Porto, Portugal*

Abstract

We study some dynamical features of certain coupled cell networks that consist of two (unidirectional or bidirectional) rings of cells coupled through a 'buffer' cell. Depending on how the rings and the buffer cell are coupled, the full network may have a non-trivial group of symmetries or a nontrivial group of 'interior' symmetries. This group is $\mathbf{Z}_p \times \mathbf{Z}_q$ in the unidirectional case and $\mathbf{D}_p \times \mathbf{D}_q$ in the bidirectional case. We are interested in finding quasi-periodic motion in these networks, motivated by an example presented by Golubitsky, Nicol and Stewart (Some curious phenomena in coupled cell systems, *J. Nonlinear Sci.* **14** (2) (2004) 207–236). In the examples considered here, we obtain quasi-periodic states through a sequence of Hopf bifurcations. Interestingly, we observe relaxation oscillation phenomena appearing further away from the last Hopf bifurcation point. We use XPPAUT and MATLAB to compute numerically the relevant states.

Key words: Quasi-periodic motion, coupled cell networks, Hopf bifurcation, relaxation oscillations
PACS: 02.60.-x, 05.45.-a, 47.52.+j

1. Introduction

Networks of dynamical systems arise in many areas of science such as biology, economics, physics and ecology. See for example Strogatz [25], Wang [27], Stewart [23], Lieberman et al. [21], Boccaletti et al. [9], Alon [3], Albert et al. [2], Watts et al. [28], Milo et al. [22], and references therein. Several general formal theories have emerged and aiming to relate the dynamics of the networks and the network structure. We follow here the theory of coupled cell networks developed in Stewart et al. [24] and Golubitsky et al. [19]. For a survey see Golubitsky and Stewart[16]. In this theory, networks of dynamical systems are idealized through coupled cell networks – directed graphs where the nodes represent the individual systems and the edges the couplings between cells. The idea is that the graph abstracts important properties of the systems. Certain dynamical phenomena such as synchronization, phase-locking, quasi-periodic states, synchronized chaos, recurrent behaviour, etc, are common in networks of dynamical systems and the architecture of the network (graph) plays an important role in the appearance of such phenomena. See for example Aguiar et al. [1], Ashwin et al. [7, 8] and Golubitsky et al. [13].

In this paper we consider networks consisting of two (unidirectional or bidirectional) (see Figure 1) rings coupled through a 'buffer' cell, exhibiting two types of architecture: 'exact symmetry' and 'interior symmetry' (see Figure 2). Specifically, we study periodic and quasi-periodic solutions arising through Hopf bifurcations in the coupled cell systems associated to the networks with the above architecture.

*Corresponding author.
Email addresses: antoneli@fc.up.pt (Fernando Antoneli), apdias@fc.up.pt (Ana Paula S. Dias), cpinto@fc.up.pt (Carla M.A. Pinto)
URL: http://www.fc.up.pt/cmup/apdias (Ana Paula S. Dias), http://www.fc.up.pt/pessoas/cpinto (Carla M.A. Pinto)
[1] CMUP is supported by FCT through the programmes POCTI and POSI, with Portuguese and European Community structural funds.
[2] The work of Fernando Antoneli is supported by FCT grant SFRH/BPD/34534/2006.

Recall that a symmetry of a network represented by a directed graph is a permutation of the nodes (cells) that preserves the edges (arrows). The notion of interior symmetry, recently introduced by Golubitsky *et al.* [14], generalizes the usual definition of symmetry. The schematic diagram on the right of Figure 2 is an example of a network with interior symmetry. Observe that if we delete the arrows directed from the rings to the 'buffer' cell then we obtain the schematic diagram on the left of Figure 2 which is an example of a network with exact symmetry (assuming that the arrows directed from the buffer cell to the rings respect the symmetry of the rings).

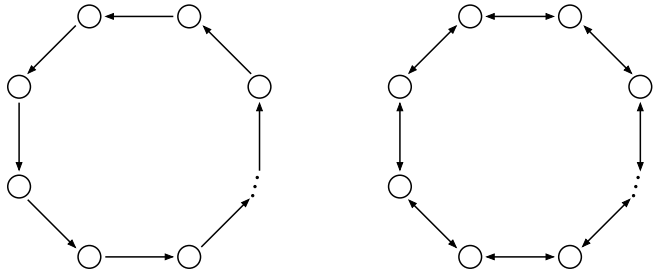

Figure 1: Schematic diagram of rings of n coupled cells. (Left) Unidirectional ring with $\mathbf{Z}_n$ symmetry. (Right) Bidirectional ring with $\mathbf{D}_n$ symmetry.

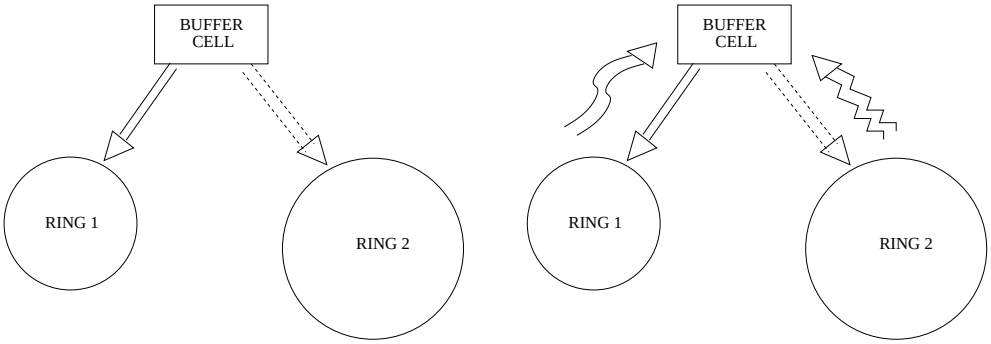

Figure 2: Schematic diagram of networks composed by two rings coupled through a buffer cell. (Left) The arrows directed from the buffer cell to the rings represent couplings that respect the symmetry of the rings, therefore the full network has symmetry $\Gamma_1 \times \Gamma_2$ where Γ_i is the symmetry group of ring i. (Right) The arrows directed from the rings to the buffer cell represent couplings that break the symmetry of the rings, therefore the full network has interior symmetry $\Gamma_1 \times \Gamma_2$ where Γ_i is the symmetry group of ring i.

We consider four networks that represent the abstract framework presented above. The first two examples are networks of two unidirectional rings, in which the first ring consists of three cells and the second ring of five cells, see Figure 3. The network in Figure 3(a) has $\mathbf{Z}_3 \times \mathbf{Z}_5$ exact symmetry and the network in Figure 3(b) has $\mathbf{Z}_3 \times \mathbf{Z}_5$ interior symmetry. The remaining networks are similar to these where now the cells in the two rings are coupled bidirectionally, see Figure 4. These latter networks have $\mathbf{D}_3 \times \mathbf{D}_5$ exact symmetry (Figure 4(a)) and $\mathbf{D}_3 \times \mathbf{D}_5$ interior symmetry (Figure 4(b)), respectively. Observe that network in Figure 3(a) is the result of ignoring the couplings from the x_i and the y_j cells to the buffer cell in the network in Figure 3(b), similarly for the networks in Figures 4(a)-(b).

It is known that symmetric ODE's exhibit robust patterns of oscillations which possess spatio-temporal symmetries. In Golubitsky *et al.* [17] it is shown how to determine and classify all permitted types of spatio-temporal symmetry that a periodic solution of a system of ODE's, with symmetry group Γ, can robustly support in terms of pairs of subgroups of Γ. This is called *H/K-Theorem*.

The first question that comes to mind is: Which of these periodic solutions can be obtained by Hopf bifurcation? The answer to this question is that not all types of spatio-temporal symmetry will arise in a Hopf bifurcation, however if one considers secondary (tertiary, etc.) Hopf bifurcations then it may be possible

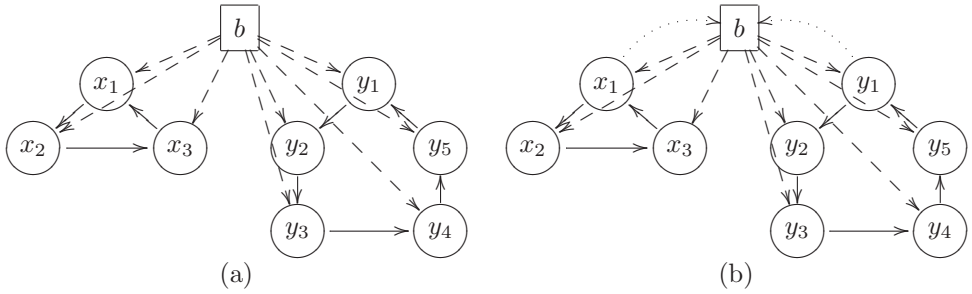

Figure 3: Networks of two coupled unidirectional rings, one with three cells and the other with five, connected through a buffer cell b. The network on the left (a) has exact $\mathbf{Z}_3 \times \mathbf{Z}_5$-symmetry whereas the network on the right (b) has interior $\mathbf{Z}_3 \times \mathbf{Z}_5$-symmetry.

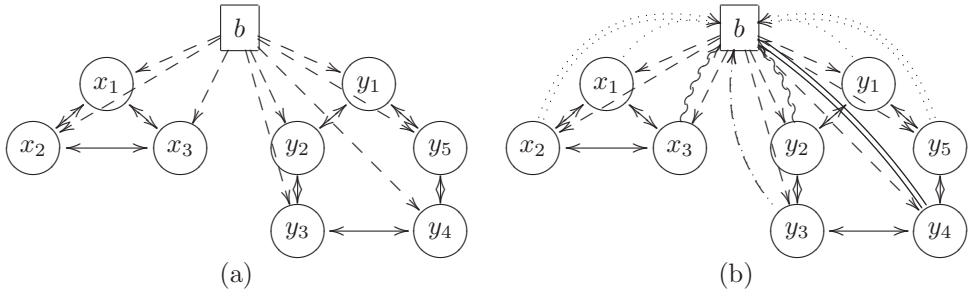

Figure 4: Networks of two coupled bidirectional rings, one with three cells and the other with five, connected through a buffer cell b. The network on the left (a) has exact $\mathbf{D}_3 \times \mathbf{D}_5$-symmetry whereas the network on the right (b) has interior $\mathbf{D}_3 \times \mathbf{D}_5$-symmetry.

that the answer is 'all solutions'. For example, in [17] there are several examples of networks displaying periodic solutions exhibiting spatio-temporal symmetries obtained through a secondary Hopf bifurcation, but would not appear in a primary Hopf bifurcation. Recently, Filipsky [12] has addressed this question in the context of equivariant dynamical systems with finite abelian symmetry and gives necessary and sufficient conditions in order to obtain a periodic solution with prescribed spatio-temporal symmetry by a *primary* Hopf Bifurcation.

Motivated by this difficult question, we have looked at some simple examples of networks with symmetry which could indicate a possible approach. In the course of our investigation we came across several other questions which are interesting by themselves and maybe relevant to the above problem. In this paper we further explore some of our findings that were already reported in Antoneli, Dias and Pinto [5, 6].

In part, our choice of examples was motivated by some of the phenomena presented by Golubitsky *et al.* [13], where a quasi-periodic motion was observed in a numerical simulation of a coupled cell network of the same type as considered here with interior symmetry. By further exploring their example, numerically, we propose a bifurcation scenario where this quasi-periodic behaviour is obtained through a sequence of Hopf bifurcations. The next step was to consider other network examples with similar structure in order to inspect if the same behaviour could occur and through a similar mechanism.

We conclude that the kind of network architecture studied here favors the appearance of quasi-periodic states. Moreover, several interesting questions and conjectures have arisen:

(1) When does a secondary Hopf bifurcation produces a quasi-periodic motion and when does it produces a periodic solution in the network?

(2) The presence of symmetry (exact or interior) constrains the dynamical behavior of the cells in each of the rings, but the structure of the vector field seems to select the periodicity or quasi-periodicity of the global solution of the network. More specifically, we believe that resonance is strongly dependant on the choice of the vector field.
(3) Another interesting phenomena observed is the appearance of relaxation oscillations, after a sequence of Hopf bifurcations, that seems to be explained by the network structure. This structure imposes a symmetry group that is a direct product of two (interior) symmetry groups, each of which is a symmetry group of a distinguished sub-network. Moreover, it is surprising to observe this type of behavior in these coupled systems since they are not *a priori* multiple time scales systems, where these solutions frequently occur (Krupa and Szmolyan [20]). Can this relaxation oscillation phenomena be explained in the context of fast-slow systems through a canard explosion?
(4) In these questions, the type of symmetry, either exact or interior, does not seem to affect in an essential way the answer to these questions.

2. Network Formalism

Recently, a new framework for the dynamics of networks has been proposed, with particular attention to patterns of synchrony and associated bifurcations. See Stewart, Golubitsky and Pivato [24, 14], Golubitsky, Nicol and Stewart [13], and Golubitsky, Stewart and Török [19]. For a survey, overview and examples, see Golubitsky and Stewart [16]. Nevertheless, we shall only need a simplified version of the 'multiarrow formalism' of Golubitsky, Stewart and Török [19], called 'single arrow formalism', which we shall briefly recall in this section.

Coupled cell networks can be represented by directed graphs whose nodes (cells) are identified with dynamical systems and whose edges (arrows) represent the couplings between them. Different node/cell symbols represent distinct internal dynamics. Different couplings are drawn as different styles of edges/arrows. Figures 3 and 4, depict four examples of coupled cell networks in which the nodes are indicated by circles and squares. In Figure 3(b) there are three different types of coupling whereas in Figure 4(b) there are seven different types of couplings.

Let us consider a coupled cell network with a finite number of nodes $\mathcal{C} = \{c_1, \ldots, c_n\}$ and a finite number of edges. If c_j is a cell then the *input set* $I(c_j)$ of c_j is the set of cells whose edges are directed to c_j. A bijection $\beta : I(c_j) \to I(c_k)$ is called an *input isomorphism* from cell c_j to cell c_k if for every $d \in I(c_j)$ one has that (i) cell d and cell $\beta(d)$ have both the same *cell type*, that is, are represented by the same node symbol and (ii) the edge directed from cell d to cell c_j and the edge directed from cell $\beta(d)$ to cell c_k have the same *arrow type*, that is, are represented by the same edge symbol.

Each cell c_j has an internal phase space P_j – here we always assume that P_j is a euclidean space $\mathbf{R}^k$. Cells represented by the same symbol have identical internal phase space. The total phase space of the network being the direct product of internal phases spaces of each cell:

$$P = \prod_{i=1}^{n} P_i \ .$$

Coordinates on P_j are denoted by x_j and coordinates on P are denoted by $(x_1, \ldots, x_n)$. The state of the system at time t is $(x_1(t), ..., x_n(t))$ where $x_j(t) \in P_j$ is the state of cell c_j at time t.

A vector field f on P is called *admissible* for a network if f is compatible with the network architecture, that is, f must satisfy the two following conditions (see Golubitsky and Stewart [16] for a precise statement):

(i) each component f_j corresponding to a cell c_j is a function only of the variables associated with the cells c_k that have edges directed to c_j (domain condition),
(ii) two components f_j and f_k corresponding to cells c_j and c_k with isomorphic input sets are identical up to a suitable permutation of the relevant variables (pull-back condition).

With the definition of admissible vector field at hand, we can speak about 'robustness' of a dynamical property of a coupled cell system, namely, a property of admissible vector fields that is persistent under admissible perturbations.

2.1. Symmetry and Interior Symmetry

Coupled cell systems often possess a non-trivial group of symmetries Γ. Symmetry is an important concept in the study of networks, since it adds more constraints on the generic behavior than if there is no symmetry at all. In particular, it helps to explain some features that seem to be exotic from the point of view of general dynamical systems theory.

A symmetry of a system of differential equations is a transformation of the phase space that sends solutions to solutions. Equivalently, if we have a system of differential equations

$$\frac{\mathrm{d}x}{\mathrm{d}t} = f(x) \ ,$$

where $x \in P$ and f is a smooth vector field, then a symmetry is a linear transformation $\gamma : P \to P$ satisfying the *equivariance condition*:

$$f(\gamma x) = \gamma f(x) \, , \qquad \forall \, x \in P \ . \tag{1}$$

A symmetry of a network is a permutation γ, acting on the set of cells and on the set of arrows that preserves the network architecture, that is, for every arrow e from cell c_i to cell c_j we have that $\gamma(e)$ is an arrow from cell $\gamma(c_i)$ to cell $\gamma(c_j)$, for all $i, j = 1, \ldots, n$. The set of symmetries of a network form a group Γ, which can be regarded as a subgroup of $\mathbf{S}_n$, the full group of permutations on n symbols.

The permutation action of the symmetry group Γ of the network on the cells induces an action of the symmetry group Γ on the phase space P of the coupled cell system by permuting the cell coordinates:

$$\gamma(x_1, \ldots, x_n) = (x_{\gamma^{-1}(1)}, \ldots, x_{\gamma^{-1}(n)}) \ , \tag{2}$$

for all $\gamma \in \Gamma$ and $(x_1, \ldots, x_n) \in P$. If f is an admissible vector field then it follows from the "pull-back condition" that the equivariance condition (1) is satisfied for all $\gamma \in \Gamma$, with respect to the action given by (2). In other words,

$$\{\text{admissible vector fields}\} \subseteq \{\text{equivariant vector fields}\} \ .$$

The concept of 'interior symmetry' was introduced in Golubitsky, Pivato and Stewart [14]. It is a generalization of the notion of a symmetry of a network that singles out a new class of networks that lies between the class of general networks and the class of symmetric networks. In this case, there is a group of permutations that acts in a subset of cells (but not on the entire set of cells) and partially preserves the network structure (cell-types and edges-types).

The network in Figure 3(b) gives an example of $\mathbf{Z}_3 \times \mathbf{Z}_5$ 'interior symmetry'. This means that if we consider the sub-network formed by ignoring the couplings from cells $x_1,\ x_2,\ x_3$ to the buffer cell and from cells $y_1,\ y_2,\ y_3,\ y_4,\ y_5$ to the buffer cell, then the resulting network is $\mathbf{Z}_3 \times \mathbf{Z}_5$-exactly symmetric. Formally, we say that the network has interior $\mathbf{Z}_3 \times \mathbf{Z}_5$-symmetry on the set of cells $\{x_1, x_2, x_3, y_1, y_2, y_3, y_4, y_5\}$. Similarly, for the network in Figure 4(b). This network is $\mathbf{D}_3 \times \mathbf{D}_5$ interiorly symmetric, and by removing the arrows from the cells in the two rings to the buffer cell, the symmetry becomes exact. This is a consequence of a general characterization of a coupled cell network with 'interior symmetry' (see Proposition 3.3 in Antoneli, Dias and Paiva [4]).

2.2. Bifurcations in Coupled Cell Systems

The theory of local bifurcations of systems of ODE's with symmetry is a well established subject (see [17, 18, 15]). The main results are the Equivariant Branching Lemma and the Equivariant Hopf Bifurcation Theorem, which give sufficient conditions for the occurrence of "symmetry-breaking" bifurcations. More precisely, the Equivariant Branching Lemma ensures the existence certain of branches of equilibrium solutions bifurcating from a fully symmetric equilibrium, provided certain conditions are satisfied. Similarly, the Equivariant Hopf Bifurcation Theorem ensures the existence of branches of periodic solutions bifurcating from a fully symmetric equilibrium. In both cases, the bifurcating solutions have less symmetry than the primary equilibrium.

More recently, Golubitsky, Pivato and Stewart [14] have given "interior symmetry-breaking" analogs of the Equivariant Branching Lemma and the Equivariant Hopf Bifurcation Theorem. The analogue of the Equivariant Branching Lemma is a natural generalisation of the symmetric case, whereas their analogue for the Equivariant Hopf Theorem imposes rather restrictive features. Specifically, it provides states whose linearization on certain subsets of cells, near bifurcation, are superpositions of synchronous states with states having *spatial symmetries*. Antoneli, Dias and Paiva [4] extend the result of Golubitsky, Pivato and Stewart, giving a full analogue of the Equivariant Hopf Theorem for networks with interior symmetry. Their result provides states whose linearization on certain subsets of cells, near bifurcation, are superpositions of synchronous states with states having *spatio-temporal symmetries*.

Since we are interested here only in the Hopf bifurcation case, we shall recall the main ideas of the Equivariant Hopf Bifurcation Theorem and its interior symmetry version.

Suppose we have a smooth one-parameter family of ODE's

$$\frac{\mathrm{d}x}{\mathrm{d}t} = f(x,\lambda)\ , \tag{3}$$

where $x \in P$ and $f(\cdot,\lambda)$ is equivariant with respect to an action finite group Γ. Assume that $f(0,\lambda) \equiv 0$. Let $\lambda = 0$ be a parameter value where (3) undergoes a local bifurcation. This means that the linearization $L = (\mathrm{d}f)_{(0,0)}$ of f about $(0,0)$ has one or more critical eigenvalues. In the case we are concerned here, all the critical eigenvalues are purely imaginary. Let $E^c(L)$ denote the corresponding center subspace, that is, the subspace generated by all generalized eigenvectors corresponding to the critical eigenvalues.

Now, in several important cases considered in equivariant bifurcation theory, one has a unique decomposition

$$P = V_0 \oplus V_1 \oplus \ldots \oplus V_k\ ,$$

where, $V_0 = \mathrm{Fix}_P(\Gamma)$ and for $j = 1,\ldots,k$ each V_j is of one of three types: (i) V_j is absolutely irreducible – the only linear mappings commuting with Γ are the real scalar multiples of the identity, (ii) V_j is non-absolutely irreducible or (iii) $V_j = W_j^+ \oplus W_j^-$, with W_j^+, W_j^- both absolutely irreducible and mutually Γ-equivalent (see [17, 18]). Here,

$$\mathrm{Fix}_P(\Gamma) = \{x \in P : \gamma x = x\,,\ \forall\,\gamma \in \Gamma\}$$

denotes the *fixed-point subspace* of Γ, which is the largest Γ-invariant subspace of P where Γ acts trivially. In the (ii) and (iii) cases, we say that V_j is Γ-*simple*.

On the other hand, one of the consequences of the equivariance condition for (3) is that $E^c(L)$ is a Γ-invariant subspace of P. Furthermore, it can be shown that, generically, in the Hopf case, when all the critical eigenvalues are purely imaginary, $E^c(L)$ should be a Γ-simple subspace (see [17, 18]). In particular, this implies that there is only one pair of purely imaginary eigenvalues (perhaps) with high multiplicity and thus coordinates can be chosen such that

$$L^c = L|_{E^c(L)} = \begin{pmatrix} 0 & -I \\ I & 0 \end{pmatrix}$$

if the purely imaginary eigenvalues are rescaled to $\pm i$. Therefore, there is a rather small list of candidates for the center subspace $E^c(L)$ of an equivariant bifurcation problem under the above circumstances. Whenever, $E^c(L)$ is a non-trivial ($E^c(L) \neq \mathrm{Fix}_P(\Gamma)$) Γ-simple subspace we say that we have a *symmetry-breaking Hopf bifurcation*.

From now on we assume that $E^c = E^c(L)$ is a Γ-simple subspace. Since L^c commutes with Γ, we may consider the action of $(\gamma,\theta) \in \Gamma \times \mathbf{S}^1$ on E^c defined by

$$(\gamma,\theta)\cdot x = \mathrm{e}^{-\theta L^c}\gamma x = \gamma \mathrm{e}^{-\theta L^c} x\,, \qquad \forall\, x \in E^c\ .$$

A subgroup $\Sigma \subset \Gamma \times \mathbf{S}^1$ is called $\mathbf{C}$-*axial* (on $E^c(L)$) if

$$\dim \mathrm{Fix}_{E^c(L)}(\Sigma) = 2\ .$$

Theorem 2.1 (Equivariant Hopf Theorem [18]). *Consider a smooth one-parameter family of ODE's*

$$\frac{\mathrm{d}x}{\mathrm{d}t} = f(x,\lambda) \ ,$$

such that $f(0,\lambda) \equiv 0$ *and* $f(\cdot,\lambda)$ *is equivariant with respect to a finite group* Γ*. Suppose that one has a symmetry-breaking Hopf bifurcation when* $\lambda = 0$*, that is, the center subspace* E^c *of* $L = (\mathrm{d}f)_{(0,0)}$ *is non-trivial and* Γ*-simple. Assume the* eigenvalue crossing condition*: the critical eigenvalues* μ *of* L *extend uniquely and smoothly to eigenvalues* $\mu(\lambda)$ *of* $(\mathrm{d}f)_{(x_0,\lambda)}$ *for* λ *near* 0 *and*

$$\frac{\mathrm{d}}{\mathrm{d}\lambda}\,\mathrm{Re}(\mu(\lambda))\bigg|_{\lambda=0} \neq 0 \ .$$

Then for each $\mathbf{C}$*-axial subgroup* $\Sigma \subset \Gamma \times \mathbf{S}^1$ *on* E^c *there exists a unique branch of periodic solutions with period* $\approx 2\pi$ *emanating from the origin and with spatio-temporal symmetries* Σ*.*

In order to state an analogue theorem in the interior symmetry context we need to assume that the system (3) is a coupled cell system associated to a network with interior symmetry Γ. The main difference from the previous situation is that f is no longer Γ-equivariant. However, since Γ acts non-trivially on a subset $\mathcal{S} \subset \mathcal{C}$ of the cells, we have a natural decomposition of the phase space P as

$$P = P_{\mathcal{S}} \oplus P_{\mathcal{C}\setminus\mathcal{S}} \ ,$$

where

$$P_{\mathcal{S}} = \prod_{i\in\mathcal{S}} P_i \qquad \text{and} \qquad P_{\mathcal{C}\setminus\mathcal{S}} = \prod_{i\in\mathcal{C}\setminus\mathcal{S}} P_i \ ,$$

with coordinates $(x_{\mathcal{S}}, x_{\mathcal{C}\setminus\mathcal{S}})$. If $f : P \to P$ is an admissible vector field then we can write $f = (f_{\mathcal{S}}, f_{\mathcal{C}\setminus\mathcal{S}})$ where $f_{\mathcal{S}} : P \to P_{\mathcal{S}}$ and $f_{\mathcal{C}\setminus\mathcal{S}} : P \to P_{\mathcal{C}\setminus\mathcal{S}}$. The pull-back condition for the coupled cell system implies that

$$\gamma f_{\mathcal{S}}(x_{\mathcal{S}}, x_{\mathcal{C}\setminus\mathcal{S}}) = f_{\mathcal{S}}(\gamma x_{\mathcal{S}}, x_{\mathcal{C}\setminus\mathcal{S}}) \ , \tag{4}$$

for all $\gamma \in \Gamma$.

On the other hand, we may introduce another set of coordinates on P, adapted to the action of the interior symmetry group Γ. First of all it can be shown that the subspace $\mathrm{Fix}_P(\Gamma)$ is flow-invariant (see [4, 14]). Since $\mathrm{Fix}_P(\Gamma)$ is Γ-invariant and Γ acts trivially on the cells in $\mathcal{C}\setminus\mathcal{S}$ we have that $P_{\mathcal{C}\setminus\mathcal{S}} \subset \mathrm{Fix}_P(\Gamma)$.

The action of the group Γ on $\mathcal{S}$ induces a decomposition

$$\mathcal{S} = \mathcal{S}_1 \cup \ldots \cup \mathcal{S}_k \ ,$$

where the sets $\mathcal{S}_i$ $(i = 1, \ldots, k)$ are the orbits of the Γ-action. Let $U = \mathrm{Fix}_P(\Gamma)$ and

$$W = \left\{ x \in P \ : \ x_c = 0 \ \ \forall\, c \in \mathcal{C}\setminus\mathcal{S} \ \text{ and } \sum_{s\in\mathcal{S}_i} x_s = 0 \ \text{ for } 1 \leqslant i \leqslant k \right\} \ .$$

Since W is a Γ-invariant subspace of $P_{\mathcal{S}}$ and $W \cap U = \{0\}$ we can decompose the phase space P as a direct sum of Γ-invariant subspaces

$$P = U \oplus W \ .$$

By further decomposing W into irreducible components under the Γ action we arrive at a decomposition

$$P = U_0 \oplus U_1 \oplus \ldots \oplus U_k \ ,$$

where, $U_0 = U = \mathrm{Fix}_P(\Gamma)$. Once again, in several important cases we have that each U_j with $j = 1, \ldots, k$ is of one of three types: (i) U_j is absolutely irreducible, (ii) U_j is non-absolutely irreducible or (iii) $U_j = W_j^+ \oplus W_j^-$, with W_j^+, W_j^- both absolutely irreducible and mutually Γ-equivalent.

Now choose a basis of P adapted to the decomposition $P = U \oplus W$ and then an admissible linear mapping L can be written as

$$L = \begin{bmatrix} A & 0 \\ C & B \end{bmatrix} ,$$

where $B = L|_U : U \to U$, $C : W \to U$ and from (4) $A : W \to W$ satisfies

$$A\,\gamma = \gamma A\,, \qquad \forall\,\gamma \in \Gamma\ .$$

The spectral properties of the linear mappings L as above are given by

Lemma 2.2 (Golubitsky *et al.*[14]). *Let $L : P \to P$ be linear mapping admissible for a coupled cell system with interior symmetry Γ. Then*

(i) The eigenvalues of L are the eigenvalues of A together with the eigenvalues of B.

(ii) A vector $u \in U = \mathrm{Fix}_P(\Gamma)$ is an eigenvector of B with eigenvalue ν if and only if u is an eigenvector of L with eigenvalue ν.

(iii) If $w \in W$ is an eigenvector of A with eigenvalue μ, then there exists an eigenvector v of L with eigenvalue μ of the form $v = w + u$, where $u \in U = \mathrm{Fix}_P(\Gamma)$.

(iv) All eigenspaces of A are Γ-invariant.

As mentioned before, in general, f is not Γ-equivariant and L does not commute with Γ. In particular, $E^c(L) \not\subset W$. However, the block matrix A does commute with Γ and thus $E^c(A) \subset W$ is Γ-invariant. Moreover, if A has purely imaginary eigenvalues there is a natural action of $\Gamma \times \mathbf{S}^1$ on $E^c(A)$, where $\mathbf{S}^1$ acts by $\exp(-\theta A)$.

We say that f undergoes an *interior symmetry-breaking Hopf bifurcation* if the following conditions hold:

(i) All the critical eigenvalues μ of L come from the Γ-equivariant sub-block A of L.

(ii) The matrix A is non-singular and (after rescaling time if necessary) all the critical eigenvalues have the form $\pm i$ and the associated center subspace is given by

$$E_i(A) = \{x \in W : (A^2 + 1)x = 0\}\ .$$

A subgroup $\Sigma \subset \Gamma \times \mathbf{S}^1$ is called *interiorly* $\mathbf{C}$*-axial* (on $E^c(A)$) if

$$\dim \mathrm{Fix}_{E^c(A)}(\Sigma) = 2\ .$$

Theorem 2.3 (Interior Symmetry Breaking Hopf Theorem [5]). *Consider a smooth one-parameter family of ODE's*

$$\frac{\mathrm{d}x}{\mathrm{d}t} = f(x, \lambda)\ ,$$

such that $f(0, \lambda) \equiv 0$ and $f(\cdot, \lambda)$ is a coupled cell system associated with a network with interior symmetry Γ. Suppose that one has an interior symmetry-breaking Hopf bifurcation when $\lambda = 0$. Assume the eigenvalue crossing condition*: the critical eigenvalues μ of L extend uniquely and smoothly to eigenvalues $\mu(\lambda)$ of $(\mathrm{d}f)_{(x_0,\lambda)}$ for λ near 0 and*

$$\frac{\mathrm{d}}{\mathrm{d}\lambda}\,\mathrm{Re}(\mu(\lambda))\bigg|_{\lambda=0} \neq 0\ .$$

Then for each interiorly **C***-axial subgroup* $\Sigma \subset \Gamma \times \mathbf{S}^1$ *on* $E^c(A)$ *there exists a unique branch of periodic solutions with period* $\approx 2\pi$ *emanating from the origin such that to lowest order in the bifurcation parameter* λ*, the solution* $x(t)$ *is of the form*

$$x(t) \approx w(t) + u(t) \ ,$$

where $w(t) = \exp(tL)w_0$ *(*$w_0 \in \mathrm{Fix}_W(\Sigma)$*) has exact spatio-temporal symmetry* Σ *on the cells in* $\mathcal{S}$ *and* $u(t) = \exp(tL)u_0$ *(*$u_0 \in \mathrm{Fix}_P(\Gamma)$*) is synchronous on the* Γ*-orbits of cells in* $\mathcal{S}$*.*

We can produce a list of all spatio-temporal patterns satisfying the conditions of the above results and that are expected to occur when one of the coupled cell systems associated to the networks of Figures 3-4 undergoes a (interior) symmetry-breaking Hopf bifurcation. In both cases the **C**-axial subgroups and the interiorly **C**-axial subgroups are the same for the networks (a) and (b). It is only the form of the solutions that depend on weather the symmetry is interior or exact.

First we observe that, since we are considering coupled cells systems the action of the groups are by permutation of coordinates. Second, in all cases, the groups in question are direct products $\Gamma = \Gamma_1 \times \Gamma_2$, with the following properties: (i) the first factor Γ_1 acts non-trivially on the subset of cells $\mathcal{R}_1$ in one of the rings and acts trivially on $\mathcal{C} \setminus \mathcal{R}_1$; (ii) the second factor Γ_2 acts non-trivially on the subset of cells $\mathcal{R}_2$ in one of the rings and acts trivially on $\mathcal{C} \setminus \mathcal{R}_2$; (iii) $\mathcal{R}_1$ and $\mathcal{R}_2$ are disjoint; (iv) the whole group $\Gamma = \Gamma_1 \times \Gamma_2$ acts trivially on $\mathcal{C} \setminus (\mathcal{R}_1 \cup \mathcal{R}_2)$. It follows then – since the action is by permuting the coordinates – that the phase space P can be decomposed as

$$P = P_0 \oplus P_1 \oplus P_2 \ ,$$

with the following properties: (i) Γ acts trivially on P_0, that is, $P_0 = \mathrm{Fix}_P(\Gamma)$; (ii) Γ_1 acts non-trivially on P_1 and acts trivially on $P_0 \oplus P_2$; (iii) Γ_2 acts non-trivially on P_1 and acts trivially on $P_0 \oplus P_1$.

Now recall that an irreducible representation of a direct product $\Gamma = \Gamma_1 \times \Gamma_2$ is a tensor product of irreducible representations of the factors. Combining this fact with our previous observations, it follows that when we decompose P into irreducible components of Γ the only components that appear are of two types: (i) a tensor product of a non-trivial irreducible representation of Γ_1 with the one-dimensional trivial representation of Γ_2; or (ii) a tensor product of a non-trivial irreducible representation of Γ_2 with the one-dimensional trivial representation of Γ_1. This fact in turn, implies that the **C**-axial subgroups of Γ in any of the Γ-simple subspaces that occur in our examples are of the form

$$\Sigma_1 \times \Gamma_2 \qquad \text{or} \qquad \Gamma_1 \times \Sigma_2 \ ,$$

where $\Sigma_i \subset \Gamma_i \times \mathbf{S}^1$ $(i = 1, 2)$ are **C**-axial subgroups.

We also need a classification of the non-trivial irreducible representations of $\mathbf{Z}_n$ and $\mathbf{D}_n$ in order to find all the possible candidates to a center subspace. In the case of $\mathbf{Z}_n$ we have that all non-trivial and faithful irreducible representations are 2-dimensional and non-absolutely irreducible [18, pg. 361].

Recall that a representation is faithful if the only element of the symmetry group that acts trivially is the identity. Therefore, all non-trivial faithful irreducible subspaces of $\mathbf{Z}_n$ are $\mathbf{Z}_n$-simple subspaces and support Hopf bifurcations. In the case of $\mathbf{D}_n$ we have that all non-trivial faithful irreducible representations are 2-dimensional and absolutely irreducible [18, pg. 368]. Therefore, the $\mathbf{D}_n$-simple subspaces are a direct sum of two copies of a non-trivial absolutely irreducible representation of $\mathbf{D}_n$ and so are 4-dimensional subspaces. Furthermore, it is possible to show that the bidirectional rings support Hopf bifurcations only if the internal phase spaces of the cells in the rings are at least 2-dimensional.

Now we can proceed to the calculation of the (interiorly) **C**-axial subgroups for all four networks depicted in Figure 3 and Figure 4. In the first case (Figure 3), we need to compute the (interiorly) **C**-axial subgroups of $\mathbf{Z}_n$ (n odd prime). This computation can be found in [18, pg. 362]. It follows that, taking into account the context described above, there is only one type of **C**-axial subgroup, which is denoted $\tilde{\mathbf{Z}}_n$. The periodic solution corresponding to this type of subgroup is called *discrete rotating wave* and has spatio-temporal symmetry generated by a rotation.

Returning to the example with $\mathbf{Z}_3 \times \mathbf{Z}_5$ (interior) symmetry, we conclude there are only two (interiorly) **C**-axial subgroups: $\tilde{\mathbf{Z}}_3 \times \mathbf{Z}_5$ and $\mathbf{Z}_3 \times \tilde{\mathbf{Z}}_5$. The solutions corresponding to these subgroups are also called *rotating waves* in the case of exact symmetry and *approximate rotating waves* in the case of interior symmetry.

Now let us describe the form of the periodic solutions corresponding to the (interiorly) **C**-axial subgroups of the networks in Figure 3. When the symmetry is exact the periodic solution of type $\tilde{\mathbf{Z}}_3 \times \mathbf{Z}_5$ is such that its components corresponding to the cells in the 3-ring are periodic and have the same wave form but they are 1/3 out of phase and the components corresponding to the cells in the 5-ring stay in equilibrium. Similarly, the periodic solution of type $\mathbf{Z}_3 \times \tilde{\mathbf{Z}}_5$ is such that its components corresponding to the cells in the 5-ring are periodic and have the same wave form but they are 1/5 out of phase and the components corresponding to the cells in the 3-ring stay in equilibrium. When the symmetry is only interior it is almost the same as in the case when it is exact, with the exception that the components that stayed in equilibrium, are now oscillating as well. In fact, in the unidirectional case they are all synchronized with the buffer cell.

In the second case (Figure 4), we need to compute the (interiorly) **C**-axial subgroups of $\mathbf{D}_n$ (n odd prime). This computation can be found in [18, pg. 368]. It follows that, taking into account the context described above, there are three types of **C**-axial subgroup: $\tilde{\mathbf{Z}}_n$, $\mathbf{Z}_2$ and $\tilde{\mathbf{Z}}_2$. The periodic solution corresponding to the first type is called *discrete rotating wave* and has spatio-temporal symmetry generated by a rotation. The periodic solution corresponding to the second type has purely spatial symmetry generated by a reflexion. The periodic solution corresponding the third type has spatio-temporal symmetry generated by a reflexion. Returning to the example with $\mathbf{D}_3 \times \mathbf{D}_5$ (interior) symmetry, we conclude that there are six (interiorly) **C**-axial subgroups: $\tilde{\mathbf{Z}}_3 \times \mathbf{D}_5$, $\mathbf{Z}_2 \times \mathbf{D}_5$, $\tilde{\mathbf{Z}}_2 \times \mathbf{D}_5$, $\mathbf{D}_3 \times \tilde{\mathbf{Z}}_5$, $\mathbf{D}_3 \times \mathbf{Z}_2$ and $\mathbf{D}_3 \times \tilde{\mathbf{Z}}_2$.

The description of the periodic solutions corresponding to the (interiorly) **C**-axial subgroups of the networks in Figure 4 is similar the the first case. We shall not need to describe all of them explicitly since in our simulations we only observe (approximate) rotating waves, which have the same form as in the case of unidirectional rings.

3. Numerical Simulations

In this section, we shall describe some numerical simulations of coupled cell systems associated with the four networks depicted in Figures 3-4, which exhibit a branching pattern similar to the schematic bifurcation diagram presented in Figure 5. The numerical simulations are performed using MATLAB [29] and XPPAUT [11].

Let us start by describing the qualitative features of the bifurcation scenario represented by Figure 5. This is a schematic bifurcation diagram of a sequence of three Hopf bifurcations where the first branch emanates from a trivial branch of steady states.

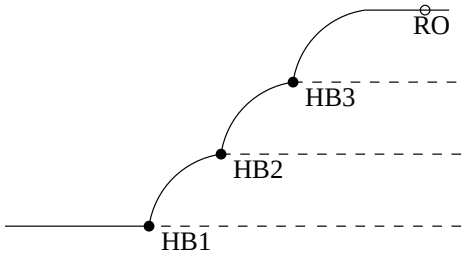

Figure 5: Schematic (partial) bifurcation diagram for the coupled cell systems considered here, near the equilibrium point. Solid lines represent stable solutions, dashed lines correspond to unstable solutions.

The solutions corresponding to the primary branch, which emanates from the trivial branch at the first Hopf bifurcation point (HB1) represented in Figure 5 can be explained using the Equivariant Hopf Theorem for coupled cell systems in the symmetric case, and the Interior Symmetry-Breaking Hopf Theorem for coupled cell systems with interior symmetry. All possible types of periodic solutions were classified in the previous section.

Recall that the (interior) symmetry groups of the networks considered here are of the form $\Gamma = \Gamma_1 \times \Gamma_2$, where Γ_1 is the symmetry group of the ring $\mathcal{R}_1$ and Γ_2 is the symmetry group of the ring $\mathcal{R}_2$. Moreover, the (interiorly) **C**-axial subgroups in our examples are of the form $\Sigma_1 \times \Gamma_2$ or $\Gamma_1 \times \Sigma_2$, where $\Sigma_i \subset \Gamma_i \times \mathbf{S}^1$ $(i = 1, 2)$ are **C**-axial subgroups. This form of the (interiorly) **C**-axial subgroups motives the following terminology:

(1) when the periodic solution corresponds to a subgroup of the form $\Sigma_1 \times \Gamma_2$ with $\Sigma_1 \subset \Gamma_1 \times \mathbf{S}^1$ a **C**-axial subgroup we say that the Hopf bifurcation has occurred in the ring $\mathcal{R}_1$.

(2) when the periodic solution corresponds to a subgroup of the form $\Gamma_1 \times \Sigma_2$ with $\Sigma_2 \subset \Gamma_2 \times \mathbf{S}^1$ a **C**-axial subgroup we say that the Hopf bifurcation has occurred in the ring $\mathcal{R}_2$.

Thus, in our simulations the primary Hopf bifurcation will occur in one of the rings, say $\mathcal{R}_1$ leading to a periodic solution with a spatio-temporal symmetry Σ_1 on the cells in $\mathcal{R}_1$ whereas the cells in $\mathcal{R}_2$ stay in equilibrium or oscillate in synchrony.

The secondary branch represented in Figure 5 is provided by a secondary Hopf bifurcation along the primary branch at the second Hopf bifurcation point (HB2). In the situation where the primary Hopf bifurcation has occurred in the ring $\mathcal{R}_1$, we expect that the secondary Hopf bifurcation is provided by the occurrence of purely imaginary eigenvalues with eigenvectors in a Γ_2-simple subspace, where Γ_2 is the symmetry group of the ring $\mathcal{R}_2$. In other words, the secondary Hopf bifurcation "occurs" in the remaing ring (the one that displayed equilibrium or total synchrony after the first Hopf bifurcation). The symmetry type of the periodic solution in the second ring $\mathcal{R}_2$ has an associated (interiorly) **C**-axial subgroup $\Sigma_2 \subset \Gamma_2 \times \mathbf{S}^1$ and so the symmetry type of the full solution has an associated (non **C**-axial) subgroup $\Sigma_1 \times \Sigma_2 \subset (\Gamma_1 \times \mathbf{S}^1) \times (\Gamma_2 \times \mathbf{S}^1)$ and is quasi-periodic.

The tertiary branch represented in Figure 5 is provided by a tertiary Hopf bifurcation along the secondary branch at the third Hopf bifurcation point (HB3). In this parameter region the solution is quasi-periodic with the same symmetry type as in the secondary branch. However, further away along this branch there is a transition to a relaxation oscillation state (RO), where now the solution is quasi-periodic and exhibits large amplitude and relaxation oscillatory behaviour.

3.1. Unidirectional Networks

For the networks in Figure 3 we consider the same coupled cell system used by Golubitsky, Nicol and Stewart [13] and studied in Antoneli *et al.* [5]. Here we summarize the key points of those works.

The internal phase space of all nine cells is the real line $\mathbf{R}$ and the internal dynamics is given by:

$$g(u) = \mu u - \frac{1}{10}u^2 - u^3 \ ,$$

where μ is a real parameter. Moreover, we assume that the coupling between all cells is linear. The full coupled cell system is

$$\begin{array}{rcll} \dot{x_j} & = & g(x_j) + c\,(x_j - x_{j+1}) + d\,b & j = 1, \ldots, 3 \\ \dot{b} & = & g(b) + \lambda\,(x_1 + y_1) & \\ \dot{y_j} & = & g(y_j) + c\,(y_j - y_{j+1}) + d\,b & j = 1, \ldots, 5 \end{array} \tag{5}$$

where $c,\ d,\ \lambda$ are real numbers, and the indexing assumes $x_4 \equiv x_1$ and $y_6 \equiv y_1$. Note that if $\lambda = 0$ then the structure of the coupled cell system (5) is consistent with the network of Figure 3(a) and thus has exact symmetry $\mathbf{Z}_3 \times \mathbf{Z}_5$; if $\lambda \neq 0$ then the coupled cell system (5) is associated to the network of Figure 3(b) and thus has interior symmetry $\mathbf{Z}_3 \times \mathbf{Z}_5$. For the numerical simulations we set $c = 0.75$, $d = 2$ and we vary the parameter $\mu \in [-1.05, 1.45]$ (going from positive values to negative values).

Figure 6 shows the time series after the primary Hopf bifurcation (HB1) in the coupled cell system 5. On the panel on the left we plot the time series for a network with exact symmetry ($\lambda = 0$) and on the right panel we plot the time series for a network with interior symmetry ($\lambda \neq 0$). The symmetry type of the periodic solution is $\mathbf{Z}_3 \times \tilde{\mathbf{Z}}_5$. In the case with exact symmetry, we observe a rotating wave on the 5-ring and

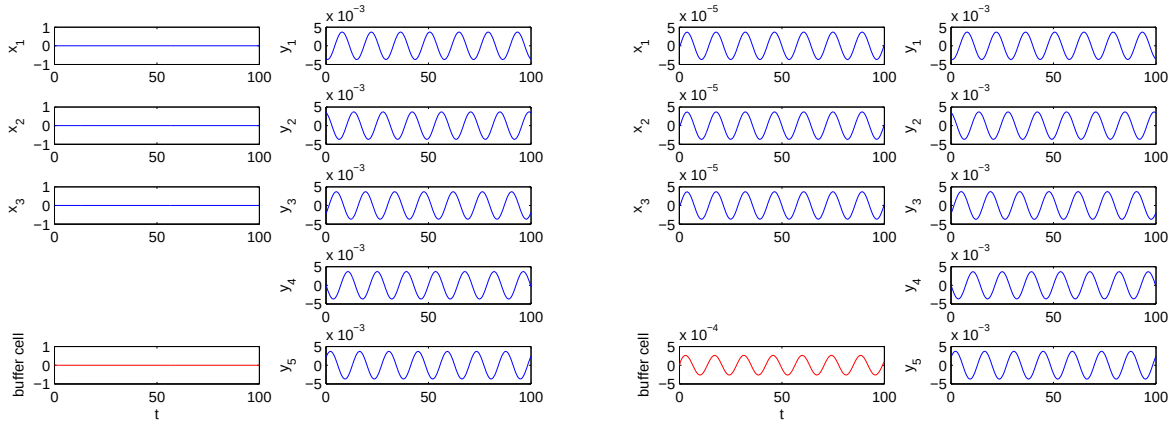

Figure 6: Simulation of the coupled system (5) with $\mathbf{Z}_3 \times \mathbf{Z}_5$ (exact and interior) symmetry. Time series from the nine cells after the first Hopf bifurcation point (HB1). (Left) Coupled cell system with exact symmetry ($\lambda = 0$). Cells in the 3-ring are at equilibrium and cells in the 5-ring display a rotating wave. (Right) Coupled cell system with interior symmetry ($\lambda \neq 0$). Cells in the 3-ring are in synchrony and cells in the 5-ring display a rotating wave.

the cells in the 3-ring stay in equilibrium. In the case with interior symmetry, we observe an approximate rotating wave in the 5-ring and the cells in the 3-ring oscillate in synchrony.

Figures 7-8 show the time series after the secondary Hopf bifurcation (HB2) in the coupled cell system 5. Here the Hopf bifurcation "occurs" in the 3-ring, leading to a $\tilde{\mathbf{Z}}_3$ rotating wave on the 3-ring. The full solution is quasi-periodic with symmetry type $\tilde{\mathbf{Z}}_3 \times \tilde{\mathbf{Z}}_5$. In Figure 7 we present the results regarding the case with exact symmetry ($\lambda = 0$) whereas in Figure 8 we present the results regarding the case with interior symmetry ($\lambda \neq 0$). On the left panel we plot the time series of all nine cells and on the right panel we plot cell x_1 versus cell y_5 showing that the solution fills in the visible region, featuring the quasi-periodicity of the solution.

It seems that there is no qualitative difference between the case with exact symmetry and the case with interior symmetry – except that, in the former case the buffer cell is in equilibrium whereas in the latter it is not. In the case with exact symmetry we have "true" rotating waves in both rings and in the case with interior symmetry they are both approximate rotating waves.

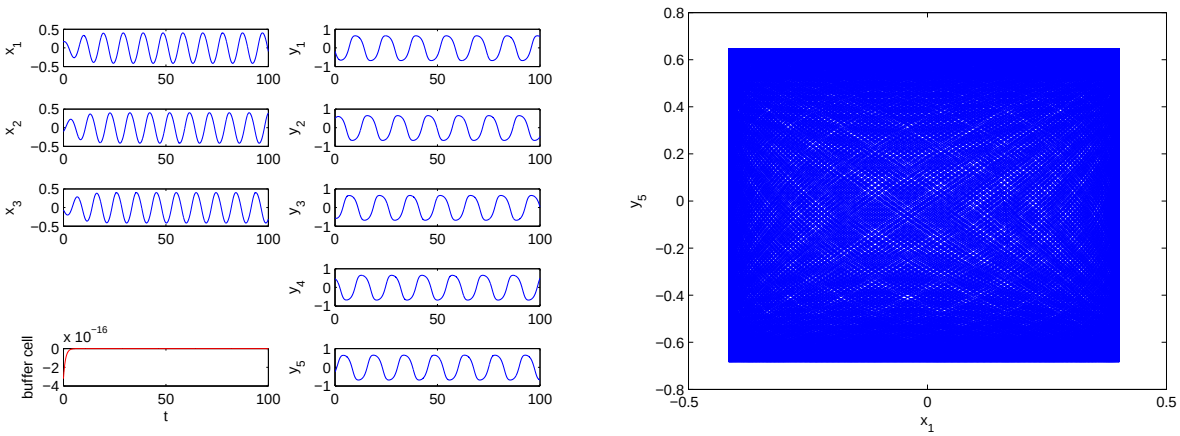

Figure 7: Simulation of the coupled system (5) with $\mathbf{Z}_3 \times \mathbf{Z}_5$ exact symmetry ($\lambda = 0$), after the second Hopf bifurcation point (HB2). (Left) Time series from the nine cells. (Right) Cell x_1 vs cell y_5.

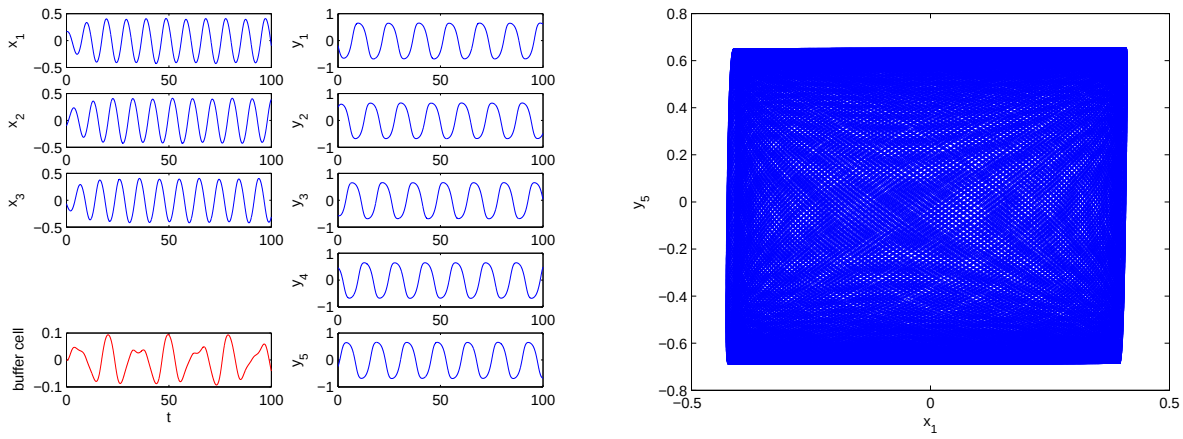

Figure 8: Simulation of the coupled system (5) with $\mathbf{Z}_3 \times \mathbf{Z}_5$ interior symmetry ($\lambda \neq 0$), after the second Hopf bifurcation point (HB2). (Left) Time series from the nine cells. (Right) Cell x_1 vs cell y_5.

Figures 9-10 show the time series further away from the tertiary Hopf bifurcation (HB3) in the coupled cell system (5). In Figures 9-10, we plot, on the left panel, the time series for the nine cells and on the right panel cell x_1 vs cell y_5, for the case with exact symmetry and the case with interior symmetry ($\lambda \neq 0$), respectively. Note that in Figure 10 the buffer cell appears to exhibit a much more complicated dynamics than the cells in the rings.

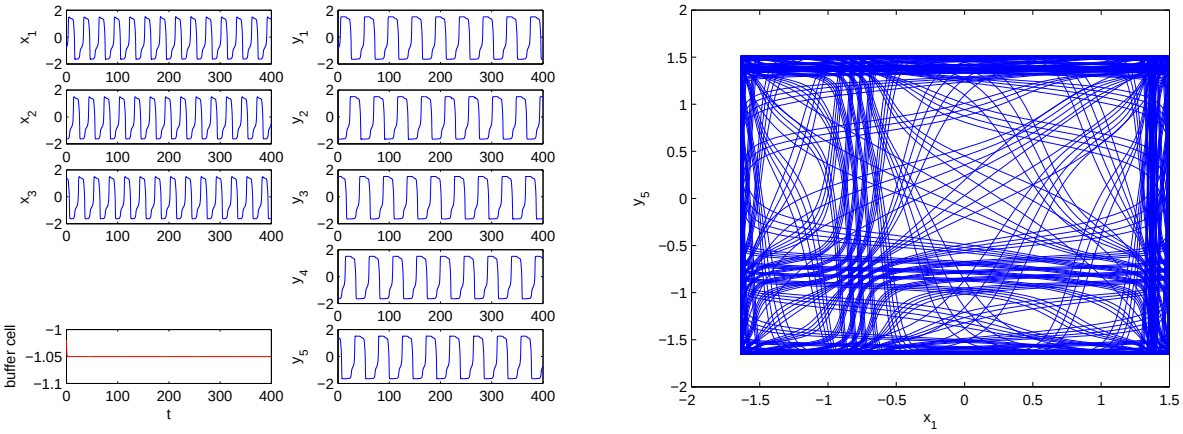

Figure 9: Simulation of the coupled system (5) with $\mathbf{Z}_3 \times \mathbf{Z}_5$ exact symmetry ($\lambda = 0$), further away from the third Hopf bifurcation point (HB3) and near the region of relaxation oscillation (RO). (Left) Time series from the nine cells. (Right) Cell x_1 vs cell y_5.

The full solution is quasi-periodic and seems to have a symmetry type $\tilde{\mathbf{Z}}_3 \times \tilde{\mathbf{Z}}_5$, that is, the time series on the 3-ring looks like a $\tilde{\mathbf{Z}}_3$ (approximate) rotating wave and the time series on the 5-ring a $\tilde{\mathbf{Z}}_5$ (approximate) rotating wave. The dynamic behavior of the coupled system (5) is qualitatively different from the one observed in Figures 7-8. Unlike in previous case (Figures 7-8), the amplitude is much higher and wave form is qualitatively different, displaying typical relaxation oscillatory features.

This curious behavior presented in Figure 10 was found by Golubitsky *et al.* [13, Section 8], where they have conjectured that the solution in the nine-dimensional phase space is either periodic of long period, or quasi-periodic. This coupled cell system was thoroughly studied by Antoneli *et al.* [5], where it was shown,

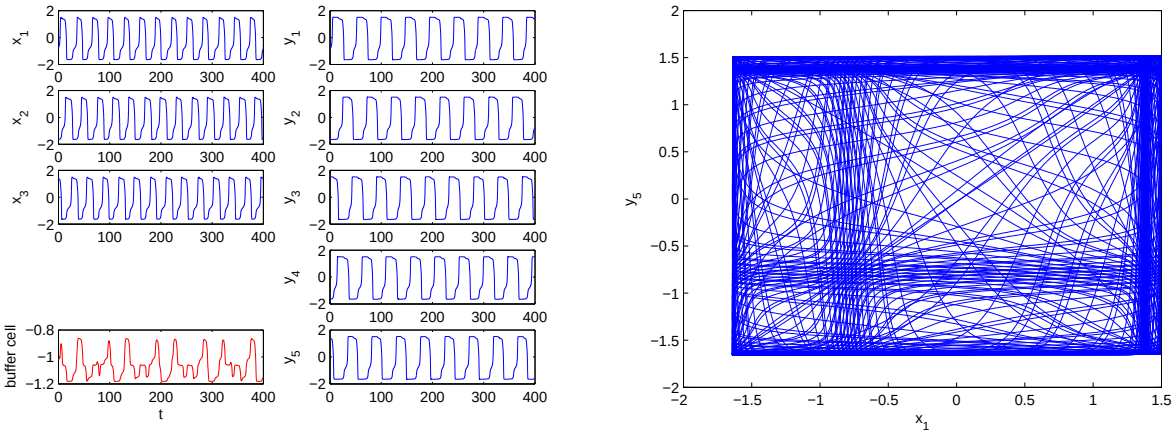

Figure 10: Simulation of the coupled system (5) with $\mathbf{Z}_3 \times \mathbf{Z}_5$ interior symmetry ($\lambda \neq 0$), further away from the third Hopf bifurcation point (HB3) and near the region of relaxation oscillation (RO). (Left) Time series from the nine cells. (Right) Cell x_1 vs cell y_5.

by numerical simulation, that the state described in Golubitsky *et al.* [13] can be obtained through a series of Hopf bifurcations starting at an equilibrium point.

3.2. Bidirectional Networks

For the networks in Figure 4, we assume the internal phase space of the nine cells to be two-dimensional $\mathbf{R}^2$. The internal dynamics is given by:

$$g(u) = a(\mu)u - \frac{1}{10}u\|u\|^4, \tag{6}$$

where $a(\mu)$ is the following 2×2 matrix depending on a real parameter μ:

$$a(\mu) = \begin{pmatrix} -0.1-\mu & -1.5 \\ 1.5 & -0.1 \end{pmatrix}.$$

Moreover, we assume that the couplings between all cells is .... The full coupled cell system is

$$\begin{aligned} \dot{x_j} &= g(x_j) + c_1\,(x_{j-1} + x_{j+1}) + c_2(\|x_j\|^2 x_{j+1}) + d\,b \qquad j = 1,\dots,3 \\ \dot{b} &= -b + \lambda\left(\textstyle\sum_{k=1}^{3} e_k x_k + \sum_{k=1}^{5} f_k y_k\right) \\ \dot{y_j} &= g(y_j) + c_1\,(y_{j-1} + y_{j+1}) + c_2(\|y_j\|^2 y_{j+1}) + d\,b \qquad j = 1,\dots,5 \end{aligned} \tag{7}$$

where c, d are real numbers and e_j $(j = 1,\dots,3)$, f_k $(k = 1,\dots,5)$ are 2×2 real matrices with $e_j \neq e_k$, $f_j \neq f_k$ for $j \neq k$. The indexing assumes $x_4 \equiv x_1$, $x_0 \equiv x_3$ and $y_6 \equiv y_1$, $y_0 \equiv y_5$. Note that if $\lambda = 0$ then the structure of the coupled cell system (7) is consistent with the network of Figure 4(a) and thus has exact symmetry $\mathbf{D}_3 \times \mathbf{D}_5$; if $\lambda \neq 0$ then the coupled cell system (7) is associated to the network of Figure 4(b) and thus has interior symmetry $\mathbf{D}_3 \times \mathbf{D}_5$. For the numerical simulations we set $c_1 = -0.1$, $c_2 = -0.01$ $d = 2$ and we vary the parameter $\mu \in [-3, 0.13]$ (going from positive values to negative values).

In Figure 11 (left), we plot the time series solution of the coupled cell system (7) for the case with exact symmetry. The solution is a rotating wave state in the 5-ring, obtained by a Hopf bifurcation (HB1), from the trivial equilibrium branch. In Figure 11 (right), we plot the time series solution of the coupled cell system (7) for the case with interior symmetry. The solution is a superposition of a rotating wave in the 5-ring and a synchronous periodic state in the 3-ring.

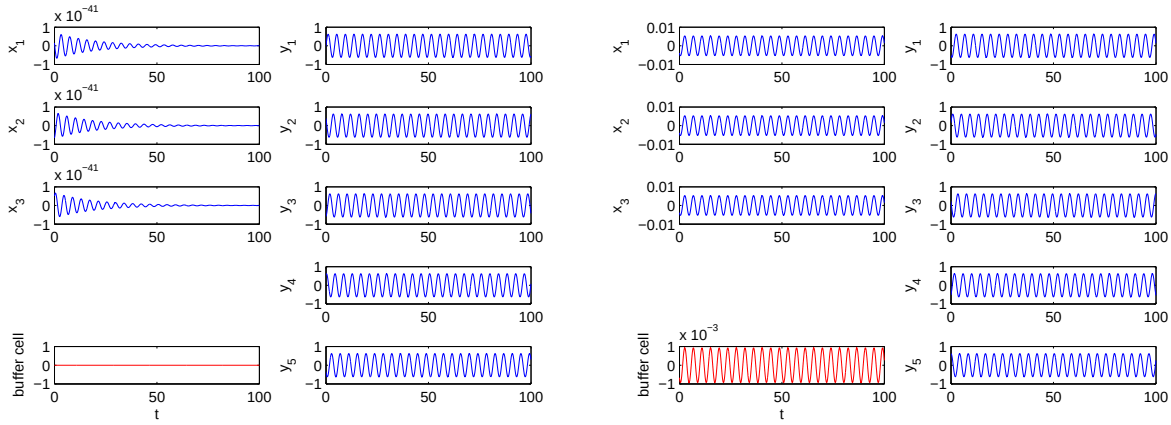

Figure 11: Simulation of the coupled system (7) with $\mathbf{D}_3 \times \mathbf{D}_5$ (exact and interior) symmetry. Time series from the nine cells after the first Hopf bifurcation point (HB1). (Left) Coupled cell system with exact symmetry ($\lambda = 0$). Cells in the 3-ring are at equilibrium and cells in the 5-ring display a rotating wave. (Right) Coupled cell system with interior symmetry ($\lambda \neq 0$). Cells in the 3-ring are in synchrony and cells in the 5-ring display a rotating wave.

By varying further the parameter μ, there is a secondary Hopf bifurcation point (HB2) where the time series of the cells in the 3-ring appear to show a $\tilde{\mathbf{Z}}_3$ rotating wave. In Figure 12, we plot, in the left panel, the individual time series of the nine cells and on the right panel we plot cell x_1 versus cells y_5, for the case with exact symmetry. In Figure 13, we plot, in the left panel, the individual time series of the nine cells and on the right panel we plot cell x_1 versus cell y_5, for case with interior symmetry. The full solution is quasi-periodic with symmetry type $\tilde{\mathbf{Z}}_3 \times \tilde{\mathbf{Z}}_5$. The quasi-periodic behavior is indicated by the non-closed curve that fills almost all the square (in both cases).

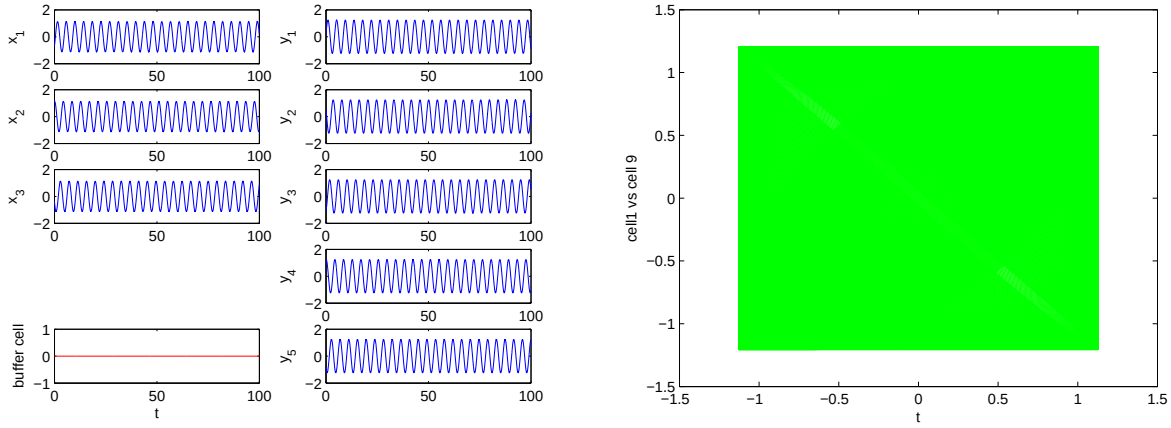

Figure 12: Simulation of the coupled system (7) with $\mathbf{D}_3 \times \mathbf{D}_5$ exact symmetry ($\lambda = 0$), after the second Hopf bifurcation point (HB2). (Left) Time series from the nine cells. (Right) Cell x_1 vs cell y_5.

Continuing the variation of parameter μ, we find a third Hopf bifurcating point (HB3). Further away from this point (HB3) – in fact, after the relaxation oscillation transition point (RO) – the dynamic behavior of the coupled system (7) is qualitatively different from the one observed in Figures 12-13. In Figure 14, we plot, in the left panel, the individual time series of the nine cells and on the right panel we plot cell x_1 versus cells y_5, for the case of exact symmetry. In Figure 15, we plot, in the top panel, the individual time series

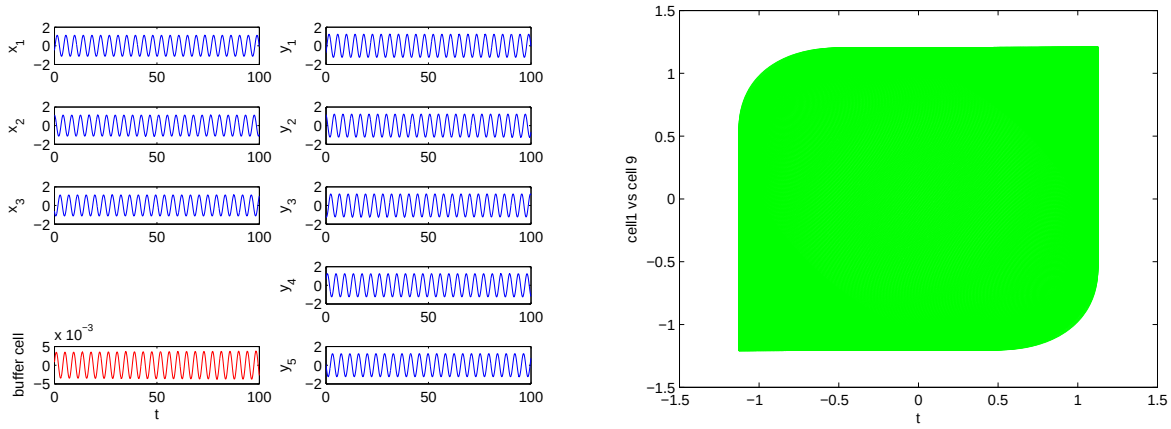

Figure 13: Simulation of the coupled system (7) with $\mathbf{D}_3 \times \mathbf{D}_5$ interior symmetry ($\lambda \neq 0$), after the second Hopf bifurcation point (HB2). (Left) Time series from the nine cells. (Right) Cell x_1 vs cell y_5.

of the nine cells and on the right panel we plot cell x_1 versus cells y_5, for the case of interior symmetry.

The time series of the cells in the 3-ring appear to show a $\tilde{\mathbf{Z}}_3$ rotating wave state and the cells in the 5-ring appear to show a $\tilde{\mathbf{Z}}_5$ rotating wave state and the full solution is quasi-periodic. However, like in the case of unidirectional ring, we observe that there is a significant growth of the amplitude and the wave form becomes qualitatively different, exhibiting typical features of a relaxation oscillation state. Note also that in Figure 15 the buffer cell appears to exhibit a much more complicated dynamics than the cells in the rings.

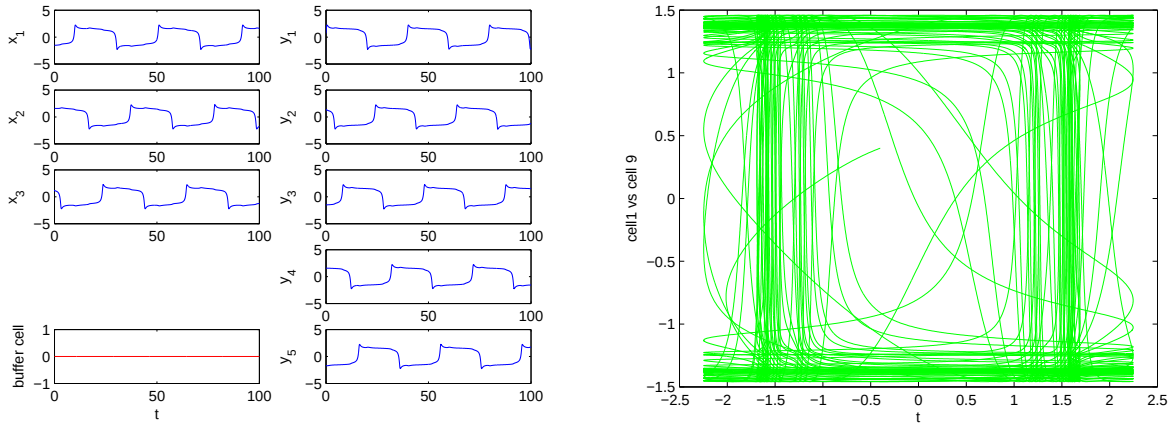

Figure 14: Simulation of the coupled system (7) with $\mathbf{D}_3 \times \mathbf{D}_5$ exact symmetry ($\lambda = 0$), further away from the third Hopf bifurcation point (HB3) and near the region of relaxation oscillation (RO). (Left) Time series from the nine cells. (Right) Cell x_1 vs cell y_5.

It is worth mentioning that in Antoneli *et al.* [6] the authors present numerical simulations of another coupled cell system associated with the networks with $\mathbf{D}_3 \times \mathbf{D}_5$ symmetry considered here, obtaining a slightly different bifurcation scenario. The main difference is that after the second Hopf bifurcation (HB2) the full state is still a periodic solution; only after the third Hopf bifurcation (HB3) a quasi-periodic behaviour is obtained. This is an indication that the structure of the vector field seems to select the periodicity or quasi-periodicity of the global solution of the network.

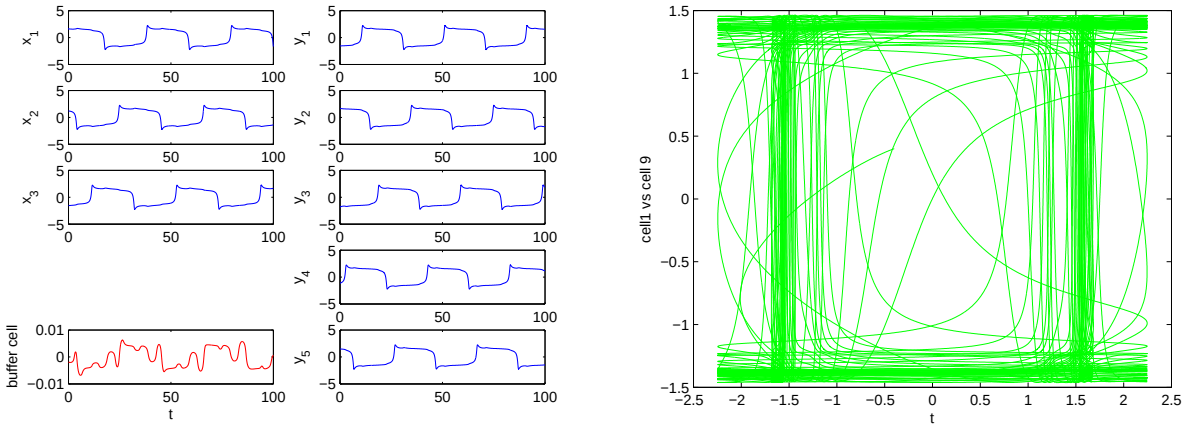

Figure 15: Simulation of the coupled system (7) with $\mathbf{D}_3 \times \mathbf{D}_5$ interior symmetry ($\lambda \neq 0$), further away from the third Hopf bifurcation point (HB3) and near the region of relaxation oscillation (RO). (Left) Time series from the nine cells. (Right) Cell x_1 vs cell y_5.

4. Conclusion

In this paper we study the dynamical behavior of networks consisting of two rings coupled through a buffer cell, that admits $\mathbf{Z}_3 \times \mathbf{Z}_5$ and $\mathbf{D}_3 \times \mathbf{D}_5$ exact and interior symmetry.

These networks exhibit a large variety of dynamic features, from states where the cells in one of the rings are at equilibrium and cells in the second ring show a rotating wave state, till a curious phenomena, namely the behaviour shown in Figures 9-10, presented by Golubitsky *et al.* [13] and studied in Antoneli *et al.* [5], for the $\mathbf{Z}_3 \times \mathbf{Z}_5$ symmetric case, and in Figures 14-15 for the $\mathbf{D}_3 \times \mathbf{D}_5$ case. The numerical simulations strongly suggest, as is the case studied in Antoneli *et al.* [5], that this dynamical feature needs a relaxation oscillation phenomena to occur. Relaxation oscillations are solutions characterized by long periods of quasi-static behavior interspersed with short periods of rapid transition. These solutions are studied in the context of the canard phenomenon [20**?** , 26].

We use XPPAUT and MATLAB to compute a partial bifurcation diagram and the corresponding dynamical states in each bifurcating branch. The bifurcation scenario is similar to the one suggested in Golubitsky *et al.* [13] and Antoneli *et al.* [5]. In particular, the curious phenomena show in Golubitsky *et al.* [13] seems to arise through a sequence of Hopf bifurcations. Additionally, the bifurcation scenario is valid to the symmetric and to the interiorly symmetric case.

In Table 1, we summarize the information, computed by XPPAUT, related to the schematic (partial) bifurcation diagram in Figure 5, and describe the dynamical behavior of the coupled cell systems at the different bifurcating branches.

References

[1] M. Aguiar, P. Ashwin, A.P.S. Dias, and M. Field. Robust heteroclinic cycles in coupled cell systems: Identical cells with asymmetric inputs, *CMUP preprint 2008-6*.

[2] R. Albert and A.-L. Barabsi. Statistical mechanics of complex networks. Rev. Mod. Phys.74 (2002) 47-97.

[3] U. Alon. Biological networks: the tinkerer as an engineer. Science 301 (2003) 1866-1867.

[4] F. Antoneli, A.P.S. Dias and R.C. Paiva. Hopf bifurcation in coupled cell networks with interior symmetries. SIAM Journal on Applied Dynamical Systems 7 (2008) 220–248.

[5] F. Antoneli, A.P.S. Dias and C.M.A. Pinto. Rich phenomena in a network of two ring coupled through a 'buffer' cell. In: *Proceedings of the 2nd Conference on Nonlinear Science and Complexity*, 2008.

[6] F. Antoneli, A.P.S. Dias and C.M.A. Pinto. New phenomena in coupled rings of cells. In: *Proceedings of the 3rd IFAC Workshop on Fractional Differentiation and its Applications*, 2008.

branch	symmetry type	μ	3-ring	5-ring	full network	Figure
trivial	$\mathbf{Z}_3 \times \mathbf{Z}_5$	1.45	equilibrium	equilibrium	equilibrium	
	$\mathbf{D}_3 \times \mathbf{D}_5$	0.13	equilibrium	equilibrium	equilibrium	
1^{st} (HB1)	$\mathbf{Z}_3 \times \mathbf{Z}_5$	1.35	equilibrium	rotating wave	periodic	6
	$\mathbf{D}_3 \times \mathbf{D}_5$	0.12	equilibrium	rotating wave	periodic	11
2^{nd} (HB2)	$\mathbf{Z}_3 \times \mathbf{Z}_5$	1.12	rotating wave	rotating wave	quasi-periodic	7,8
	$\mathbf{D}_3 \times \mathbf{D}_5$	0.00	rotating wave	rotating wave	quasi-periodic	12,13
3^{rd} (HB3)	$\mathbf{Z}_3 \times \mathbf{Z}_5$	0.51	rotating wave	rotating wave	quasi-periodic	
	$\mathbf{D}_3 \times \mathbf{D}_5$	-0.60	rotating wave	rotating wave	quasi-periodic	
3^{rd} (RO)	$\mathbf{Z}_3 \times \mathbf{Z}_5$	-0.99	relax. osc.	relax. osc.	quasi-periodic	9,10
	$\mathbf{D}_3 \times \mathbf{D}_5$	-3.00	relax. osc.	relax. osc.	quasi-periodic	14,15

Table 1: Summary of the dynamical behavior of coupled cell systems simulated in this work. In the first column we indicate some branches of solutions with the respective bifurcation points. The second, third and fourth columns show the type of asymptotic stable solutions in the rings and the full systems in the corresponding branch. See text for more details.

[7] P. Ashwin, J. Buescu and I. Stewart. Bubbling of attractors and synchronisation of oscillators. Phys. Lett. A 193 (1994) 126–139.

[8] P. Ashwin, O. Burylko and Y. Maistrenko. Bifurcation to heteroclinic cycles and sensitivity in three and four coupled phase oscillators. Phys. D 237 (4) (2008) 454–466.

[9] S. Boccaletti, V. Latora, Y. Moreno, M. Chavez and D.-H. Hwang. Complex networks: Structure and dynamics. Physics Reports 424 (2006) 175–308.

[10] W. Eckhaus. Relaxation oscillations including a standard chase on French ducks. *Asymptotic Analysis II*, Springer Lecture Notes Math. 985 (1983) 449–494.

[11] B. Ermentrout. XPPAUT® – The differential equations tool, version 5.98, 2006. (`http://www.math.pitt.edu/~bard/xpp/xpp.html`)

[12] N.T. Filipski. Periodic solutions in systems with finite abelian symmetries. PhD Thesis, University of Houston, 2008.

[13] M. Golubitsky, M. Nicol and I. Stewart. Some curious phenomena in coupled cell systems. J. Nonlinear Sci. 14 (2004) 207–236.

[14] M. Golubitsky, M. Pivato and I. Stewart. Interior symmetry and local bifurcation in coupled cell networks. Dynamical Systems 19 (2004) 389–407.

[15] M. Golubitsky and D.G. Schaeffer. *Singularities and Groups in Bifurcation Theory*, vol. 1. Applied Mathematical Sciences **51**, Springer-Verlag, New York, 1985.

[16] M. Golubitsky and I. Stewart. Nonlinear dynamics of networks: the groupoid formalism. Bull. Amer. Math. Soc. 43 (2006) 305–364.

[17] M. Golubitsky and I. Stewart. *The symmetry perspective: From Equilibrium to Chaos in Phase Space and Physical Space*. Progress in Mathematics **200**, Birkhäuser, Basel, 2002.

[18] M. Golubitsky, I.N. Stewart and D.G. Schaeffer. *Singularities and Groups in Bifurcation Theory*, vol. 2. Applied Mathematical Sciences **69**, Springer-Verlag, New York, 1988.

[19] M. Golubitsky, I. Stewart and A. Török. Patterns of synchrony in coupled cell networks with multiple arrows. SIAM J. Appl. Dynam. Sys. 4 (1) (2005) 78–100.

[20] M. Krupa and P. Szmolyan. Relaxation oscillations and canard explosion. J. Diff. Equations 174 (2001) 312–368.

[21] E. Lieberman, C. Hauert and M.A. Nowak. Evolutionary dynamics on graphs. Nature 433 (2005) 312–316.

[22] R. Milo, S.S. Shen-Orr, S. Itzkovitz, N. Kashtan and U. Alon. Network motifs: simple building blocks of complex networks. Science 298 (2002) 824-827.

[23] I. Stewart. Network opportunity. Nature 427 (2004) 601–604.

[24] I. Stewart, M. Golubitsky and M. Pivato. Symmetry groupoids and patterns of synchrony in coupled cell networks. SIAM J. Appl. Dynam. Sys. 2 (4) (2003) 609–646.

[25] S.H. Strogatz. Exploring complex networks. Nature 410 (2001) 268-276.

[26] P. Szmolyan and M. Wechselberger. Canards in $\mathbf{R}^3$. JDE 177 (2001) 419–453.

[27] X.F. Wang. Complex networks: topology, dynamics and synchronization. Int. J. Bifurc. Chaos 12 (2002) 885–916.

[28] D.J. Watts and S.H. Strogatz. Collective dynamics of 'small-world' networks. Nature 393 (1998) 440-442.

[29] The MathWorks, Inc. MATLAB®, 1994–2008. (`http://www.mathworks.com`)